Numerical Investigation of Dilution with H_2O/CO_2 and Strain Rate Effects on Laminar Diffusion Flames in Counter-flow Configuration: Analysis for Biogas-Syngas Mixture.

Rabab Belalmi [1]*; Abdelbaki Mameri[2]; Amar Hadef [3]; and Zeroual Aouachria[4].
[1,4]Applied Energy Physics Laboratory (LPEA), Department of Sciences of Matter, University of Batna1 (Algeria).
[2,3]Laboratory of Advanced Conception of Mechanical Systems and Thermo-Fluids (LCMASMTF), Department of Mechanical Engineering, University of Oum El Bouaghi (Algeria).
E-mail for the *corresponding author rabab.belalmi@univ-batana.dz
Received: 10/2023 published: 12/2023

Abstract : Environmental problems linked to the use of fossil fuels are inevitable at least in the medium term. It is therefore essential to optimize combustion systems in order to reduce harmful emissions. To achieve this goal, we combine two techniques during combustion: the use of biofuels and their dilution. The impacts of several factors, including the type of diluent (H_2O and CO_2), the volume of diluent (0% to 40%), and the site where the diluents are injected (oxidizer or fuel side), radiation losses and injection velocity (strain rate from ignition to extinction limit), are examined to obtain the maximum benefits of combustion. The oxidizer is composed of air ($0.21O_2+0.79N_2$) while the fuel is composed of an equimolar mixture of biogas and syngas (($0.25CH_4+0.25CO_2$) +($0.25H_2+0.25CO$)). The configuration of an opposed jet flame is used with constant atmospheric pressure. The chemical kinetics is described by the Gri-Mech 3.0 mechanism. The results are in good agreement with the literature data. It is found that CO_2 is more effective than H_2O in reducing maximum temperatures, NOx, CO, C_2H_2 emissions, and other soot; whether it is added to the air or fuel side. Furthermore, the maximum temperatures and extinction limits (i.e., flame resistance) for the fuel-side dilution are higher than those for the oxidant-side dilution. Nevertheless, the latter is still preferred in applications not requiring a high injection velocity. In this study, the zero-emission limit is approached for 10% of the CO_2 oxidant side dilution.

Keywords: Biogas-Syngas mixing; Diffusion flame; Flamelet model; Dilution; strain rate; Optimization.
Tob Regul Sci. ™ 2023 ;9(2): 1688-1711
DOI : doi.org/10.18001/TRS.9.2.105

Introduction

Biogas and synthesis gas are new alternative fuels. The latter is produced by the gasification of biomass or coal using Integrated Gasification Combined Cycles (IGCC) technology, which is one of the most promising technologies for future efficient and clean energy systems and produces a mixture primarily composed of H_2 and CO. Biogas is formed mostly of CH_4 and CO_2 and is generated from the anaerobic digestion of biomass. These fuels are a viable source of energy. As global energy needs and environmental concerns continue to rise [1-3], these fuels will play a greater role in tomorrow's energy production, leading to increased pollution emissions, particularly nitrogen oxides. These emissions come mainly from high-temperature processes in the industrial sectors. They have negative effects on health and the environment. Therefore, strong international commitments are needed to regulate emission ceilings. To this end, various NOx reduction technologies have been developed such as i- combustion gas recirculation (FGR) [4-6], ii- fuel injection recirculation (FIR) [7], iii- Staged combustion technology reduces NOx emissions [8, 9]. iv- selective non-catalytic reduction (SNCR) [10, 11], v- combustion without significant agitation in the combustion chamber [12], vi- rich-lean combustion techniques as a means of reducing fuel-related NOx emissions. Leonard et al [13], in a comprehensive analysis of various flame carriers with operating conditions and residence times (2–100 ms), found only that flame temperature (rather than residence time) determines NOx formation with emissions of less than 10 ppmv. This directed research into reducing the maximum flame temperature. In the category of diffusion flame burners, the flame temperature is close to its adiabatic temperature. These temperatures are high enough to oxidize atmospheric nitrogen and generate considerable harmful emissions, like NOx, which require an approach that helps in reducing NOx. Optimizing the flame temperature can involve diluting the fuel. The principal constituents of hydrocarbon combustion gases are carbon dioxide and water vapor, which are already biogas species. [14-17]. The addition of these two diluents to combustion is an effective means of reducing NOx emissions [18-24]. As a clean and efficient method, numerous research has been conducted to investigate the characteristics of a laminar flame and chemical reaction mechanisms, as well as the use of additives in the combustion of hydrocarbons, particularly methane, for a variety of applications and conditions, as carried out by [25]. In this work, the dilution chemical impact (by CO_2/H_2O/N_2) on the oxidant side is explored in the flame structure and the emission of NO in a methane-air diffusion flame against the current. From 0% to 10%, the percentage of diluents in the air stream is systematically changed. The obtained results were contrary to expectation, as it was found that the addition of CO_2 lowers the temperature (both thermally and chemically), but the addition of H_2O enhances the reaction chemically while keeping it thermally stable due to the super-balance effect. When the chemical reaction paths of nitrogen are compared between the additions of CO_2 and H_2O, it is obvious that the addition of CO_2 is more efficient in reducing NO. These findings were confirmed and explained by [26]; but this time they provided more precise and detailed explanations, as they explained the effectiveness of carbon dioxide in reducing the temperature so that when H_2O is added, the branching chain reaction $H + O_2 \rightarrow O + OH$ is significantly increased compared to

when CO_2 is added, Thus, due to the added H_2O rupture, the impacts of super-balance radicals, brought by the additional chain carriers, are much more pronounced, and accumulate by stimulating the rapid formation of NO, Consequently the total NO emission is higher than when CO_2 is added. Furthermore, the modeling of the principal nitrogen reaction paths demonstrates that the effects of the chemical overbalance of the chain-carrying radicals directly influence the thermal emission of NO in the case of the water vapor dilution, whereas the associated reactions affect the production of NO in the CO_2 addition case.

A numerical Simulation of the flame structure and the behavior of the NO emissions were carried out by [27] to capture the chemical effects of the added H_2O (fuel or oxidizer side) in the back diffusion flames. For the flow of methane, this study highlights the important role of OH radicals produced due to the chemical effects of added water on flame structure and NO emissions. It was found that the maximum flame temperature decreases with increasing molar fractions of the added H_2O. On the other hand, it should be emphasized that in all cases, dilution on the oxidant side leads to lower flame maximum temperatures than dilution on the fuel side. It was also observed that the maximum flame temperature increases due to the chemical effects of the added H_2O. Important reaction steps contributing to the production of NO were also discussed. The thermal and rapid production of NO are suppressed by the chemical effects of the added H_2O. The contribution of the reaction steps linked to the HNO intermediate species to the production of prompt NO was also underlined.

In a numerical study, the thermal, chemical, and diffusion effects of diluents (CO_2 and H_2O) on the flame temperature and the CO emission index of the CH_4-O_2 / N_2 / CO_2 / H_2O mixture of counter-current diffusion flame considerably reduce the flame temperature [2]. However, whereas H_2O has little influence on flame temperature, CO_2's chemical effect causes a considerable increase in EICO, although other H_2O and CO_2 effects reduce it slightly. CO_2 diffusion has a minor influence on flame temperature and EICO but has a major impact on their distributions.

Study [28] analyzed the effect of dilution by H_2O and CO_2, as well as the effect of strain rate on NO formation in opposed-jet H_2/CO syngas diffusion flames. The main findings showed that NO is primarily formed through the NNH intermediate pathway and thermal pathway at high strain rates. Near a strain rate of 10 s^{-1}, the highest temperature was observed, resulting in a significant dominance of NO formation via the thermal route. However, it was found that NO can be consumed through another reaction where it converts to NH via HNO, particularly for syngas rich in H_2. At lower strain rates, radiative heat loss leads to a further reduction in NO formation while another reaction becomes more important for CO-rich syngas [28]. Experimental and numerical studies on the structure of laminar co-current syngas diffusion flames [3] show that dilution with H_2O and CO_2 has the same thermal and radiative effects and decreases the maximum flame temperature but does not have the same chemical and transport effects. Furthermore, the addition of H_2O promotes the concentration of OH, which means a higher burning intensity, which leads to a decrease in the height and radius of the flame, while the addition of CO_2 decreases

the concentration of OH, increasing the length and radius of the flame. Thus, numerical and experimental results show that the dilution with H_2O and CO_2 reduces the maximum temperature of the flame, but they influence differently on the axial maximum temperature.

One of the latest published studies by Xu et al in 2021 [29], is highly relevant to the present study. In this reference, the authors confront the impact of the addition of water and carbon dioxide on the combustion and fuel sides, on the counter-current CH_4 diffusion flame, emphasizing the kinetics formation of NO. They ranked the significance of the effects of air-side and fuel-side H_2O and CO_2 dilution on NO reduction, following this order: $air-side\ CO_2\ dilution > air-side\ H_2O\ dilution >$ fuel-side H_2O dilution> CO_2fuel-side dilution.The fast pathway of NO production still plays the dominant role under current study conditions. Several other studies have also dealt with the effect of dilution with CO_2 on the shape and structure of the flame and in particular the emissions of pollutants [30-34]. Based on this literature search, diluents are ranked from the most effective to least effective as $CO_2 > H_2O > N_2 >$ Ar.

Biogas and syngas are indeed alternative fuels although their low calorific value makes them difficult to exploit because of the fragility of their flames. To overcome this problem, a study suggested mixing these two biofuels because syngas is rich in hydrogen, which is a flame-stabilizing factor for biogas. The authors evaluated the effect of composition, stretching velocity, and pressure on the thickness and structure of the counter-current biogas-syngas diffusion flame [35].

Because of the good results obtained in the reduction of pollutant emissions, several studies continued to treat this topic in “the same configuration and mixture (biogas-syngas)”. As a follow-up to their work, studies were undertaken on the effect of high stretching rates, the chemical effect of dioxide carbon in biogas, and radiation losses on the flame structure for the laminar regime [36]. Numerical studies were recently conducted to examine combustion in two-dimensional turbulent and flame-free regimes, helping to better understand the behavior of this flame by studying the formation of NOx and numerically evaluating the NOx production pathways [37, 38]. The authors of the work Benbouaziz et al [39] carried out a numerical study of the combustion in the "MILD" regime of the biogas-syngas fuel, in the configuration of the Hot Co-Flow (JCH) burner, elucidating the characteristics of the flame as a function of the Reynolds number and the concentration of oxygen.

The objective of this study is to reduce as much as possible the polluting emissions, in particular NO, considered as the current stake. To achieve this goal, we combine two techniques: the use of biofuels and combustion by dilution. The effects of three main parameters will be examined. In addition, the effects of radiation and the rate of deformation on the flame structure, and the emissions of the laminar counter-current diffusion flame of the Biogas-Syngas mixture are presented. This is done, in constant-pressure combustion systems, to define the production of NOx.

Geometry and numerical calculation strategy

The configuration of the opposite jet is widely used in numerical and experimental studies. Many fuels and oxidizers are tested by [23, 40-42]. It simplifies the flow equations and combustion structure and represents one of the simplest setups in which the diffusion flame extinction can be measured. for this reason, this configuration is chosen in this study.

The opposed jet diffusion flame configuration

The physical model considered here is a counter-flow, laminar diffusion flame stabilized near the stagnation plane of two opposing jet flows separated by a distance D = 1.5 cm, as depicted in Figure 1. In this study, the effects of radiation losses, strain rate, and dilution of combustion by injecting H_2O or CO_2 through the two jets at a volume ranging from 0% to 40% are considered. The flame structure is assumed to be uniform in the r-direction (r-direction in the figure). This assumption produces a one-dimensional flame whose characteristics are a function of x (x direction in the figure). The study of the structure of the flame is done in a cross-section of the flame (x direction).

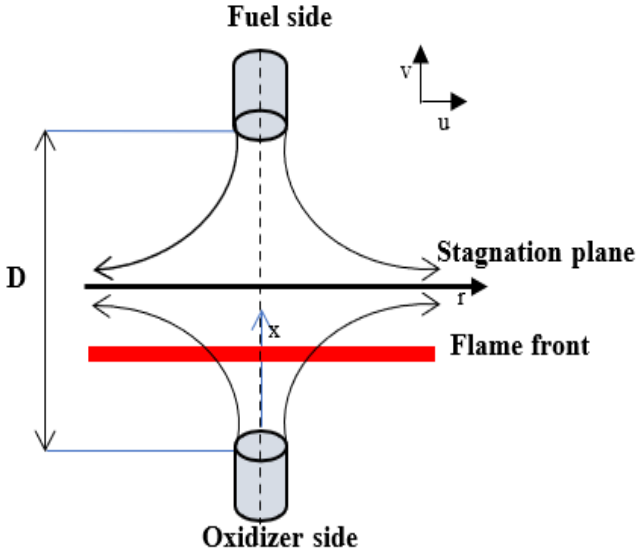

Figure 1. Counter-flow no premixed flame configuration.

Purpose of the work and operating conditions

This work aims to demonstrate the effect on the flame structure, extinction limits, temperature, and major and minor species of:

- Combustion reactants dilution by different types and volumes of the diluents. Both H_2O and CO_2 were considered with a volume varied from 0% to 40% for the fuel and oxidizer sides alternatively.
- Strain rate ranged from its low value at the ignition to the high one at the extinction of the flame.
- Losses by radiation effects were also considered.

The boundary conditions for fuel and oxidizer are:

- Atmospheric pressure P = 1 atm
- Inlet temperature for both jets is constant and equals 300 K.

- Equimolar biogas-syngas mixture (25% CH_4, 25% CO_2, 25% H_2, and 25% CO) is injected into the fuel side. Whereas, air ($0.21O_2$+$0.79N_2$) is injected in the oxidizer side.
- Dilution is practiced by substituting a volume of fuel or oxidizer with a volume β of diluent. The volumetric composition of the injected fuel is given by:

$$\left(0.25-\frac{\beta}{4}\right)CH_4+\left(0.25-\frac{\beta}{4}\right)CO_2+\left(0.25-\frac{\beta}{4}\right)H_2+\left(0.25-\frac{\beta}{4}\right)CO \quad (1)$$

or oxidizer by:

$$\left(0.21-\frac{\beta}{2}\right)O_2+\left(0.79-\frac{\beta}{2}\right)N_2 \quad (2)$$

- Where β is the volume of H_2O or CO_2 added to the fuel or oxidizer side, exactly β ranges from 0% to 40% with a step of 5%.
- Injection velocities are equal for both fuel and oxidizer, and the strain rate is calculated by [31]:

$$a=\frac{2(-v_0)}{D}\left[1+\frac{v_F}{v_0}\sqrt{\frac{\rho_F}{\rho O}}\right] \quad (3)$$

Were v_0, v_F, ρ_0, and ρ_F are respectively the oxidizer injection velocity, fuel injection velocity, oxidizer density, and fuel density, and D is the distance between the two injectors. The calculation is made for the case of the flame with and without losses by radiation. Species molecular diffusion is approximated by an averaged coefficient for all the species.

- Chemical kinetics is described by the Gri-Mech 3.0 reaction mechanism.

Governing equations of the problem

Since most combustion processes involve fluid flow, heat transfer, and species production by chemical reactions; fluid mechanics, heat transfer, and chemical kinetics principles are used to characterize combustion processes. The governing equations on this problem are [41]:

$$\frac{\partial \rho u}{\partial x}+\frac{1}{r}\frac{\partial(\rho v r)}{\partial r}=0 \quad (4)$$

$$\frac{d}{dx}\left(\frac{\rho u v}{r}\right)=-\frac{1}{r}\frac{\partial P}{\partial r}+\frac{d}{dx}\left(\mu\frac{d}{dx}\left(-\frac{\rho v}{r}\right)\right)-3\frac{\rho v^2}{r^2} \quad (5)$$

$$\rho u\frac{dY_k}{dx}+\frac{d}{dx}(\rho Y_K V_K)-\dot{\omega}_K M_K=0 \quad (6)$$

$$\rho u\frac{dT}{dx}-\frac{1}{C_P}\frac{d}{dx}\left(\lambda\frac{dT}{dx}\right)+\frac{\rho}{C_p}\sum_k Cp_k\,Y_k\,V_k\frac{dT}{dx}+$$
$$+\frac{1}{C_p}\sum_k h_k\,\dot{\omega}_k+\frac{1}{C_p}\left[4\sigma p\sum_j X_J\,a_i\,(T^4-T_f^4)\right]=0 \quad (7)$$

Where the mass diffusion velocity is:

$$V_k=\frac{1}{X_k\overline{M}}\sum_{j=1}^{k}M_j D_{k,j}\frac{dX_j}{dx}-\frac{D_k^T}{\rho_k}\frac{1}{T}\frac{dT}{dx} \quad (8)$$

Where $D_{k,j}$ and D_k^T are multicomponent and thermal diffusion coefficients, respectively.

The last term in equation (8) represents radiation loss resulting from the optically thin model. In this term, σ, p, x_j, and T_f are the Stefan-Boltzmann constant, pressure, x_j the species mole fraction, and far-field temperature, respectively the a_i constants are polynomial factors for Planck mean absorption coefficients. The considered gaseous species that participate in radiation are CH_4, CO, CO_2, and H_2O. The partial differential equations with their appropriated boundary conditions will be solved by the Chemkin program.

Calculations and results

Numerical procedure validation

To now day, there is no experimental research that treats the effects of dilution or more precisely the effect of the injection site of the diluent (fuel or oxidant side) on the maximum temperature and the pollutant emissions of the counterflow diffusion flame of the biofuel's mixture (biogas-syngas). In this way, the experimental results of Lim et al. [42] are used to validate the results obtained in the present study. With the same operating conditions which are: the distance between the two ducts D=1.5cm, the injector velocities are equal to 70 cm/s, injection temperature T=300K, and atmospheric pressure P=1 atm. Experiments were performed with methane (Airco Gas and Gear, 99% methane) introduced from the bottom duct and air introduced from the top duct.

Figure 2 presents a comparison between numerical calculations and experimental data of gas species (CH_4, O_2, N_2, CO_2, CO, H_2, C_2H_2, C_2H_4), using Chemkin and GRI-Mech 3.0 mechanisms. An excellent agreement between simulation and measurement data for CH_4, O_2 and N_2 is shown in Fig. 2(a), and a good agreement for CO_2, CO, and H_2 in Fig. 2 (b) but only a low agreement is noted for C_2H_2 and C_2H_4 as illustrated in Fig. 2(c).

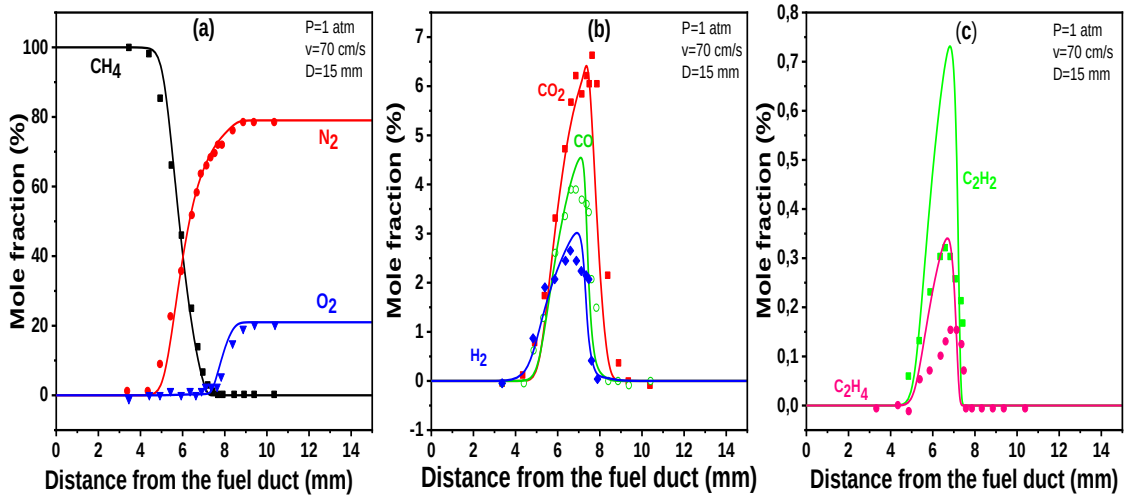

Figure 2. Comparison between predictions and experimental data; (a) CH_4, O_2, and N_2, (b) CO_2, CO, H_2 and (c) C_2H_2 , C_2H_4 (▶■● experimental results [42] − computations).

Solution of the problem

In this study, the dilution is operated on the two jets. The computed flame compositions and their denominations are given in Tables 1 and 2.

Table 1. The composition and denominations of the flames diluted on the fuel side.

Flames denominations	Compositions of the flames				i=1 dilution with H_2O i=2 dilution with CO_2	Some
	CH_4	CO_2	H_2	CO		
F1D0	0.25	0.25	0.25	0.25	0	1
FiDF5%	0.2375	0.2375	0.2375	0.2375	0.05	1
FiDF10%	0.225	0.225	0.225	0.225	0.10	1
FiDF15%	0.2125	0.2125	0.2125	0.2125	0.15	1
FiDF20%	0.2	0.2	0.2	0.2	0.20	1
FiDF25%	0.1875	0.1875	0.1875	0.1875	0.25	1
FiDF30%	0.175	0.175	0.175	0.175	0.30	1
FiDF40%	0.15	0.15	0.15	0.15	0.40	1

Table 2. The composition and denominations of the flames diluted on the oxidant side.

Flames denominations	Compositions of the flames		i=1 dilution with H_2O i=2 dilution with CO_2	Some
	O_2	N_2		
F1D0	0.21	0.79	0	1
FiDOX5%	0.185	0.765	0.05	1
FiDOX10%	0.16	0.74	0.10	1
FiDOX15%	0.135	0.715	0.15	1
FiDOX20%	0.11	0.69	0.20	1
FiDOX25%	0.085	0.665	0.25	1
FiDOX30%	0.06	0.64	0.30	1
FiDOX40%	0.01	0.59	0.40	1

Flame structure

To illustrate the important role of strain rate and dilution by H_2O and CO_2 in the reduction of the maximum flame temperature and emissions; three different strain rates were considered ($a=15s^{-1}$ near the ignition, $a=30s^{-1}$ near the region, when variables take their maximal values and $a=400s^{-1}$ near the extinction) for the following cases of the mixture, biogas-syngas with and without dilution (F1D0, F1DF5%, F1DF40%, F2DF5%, F2DF40%, F1DOX5%, F1DO10%,

F2DOX5%, F2DOX10%) in the function of the distance X between the two ducts, at ambient pressure of 1atm and including radiation heat losses.

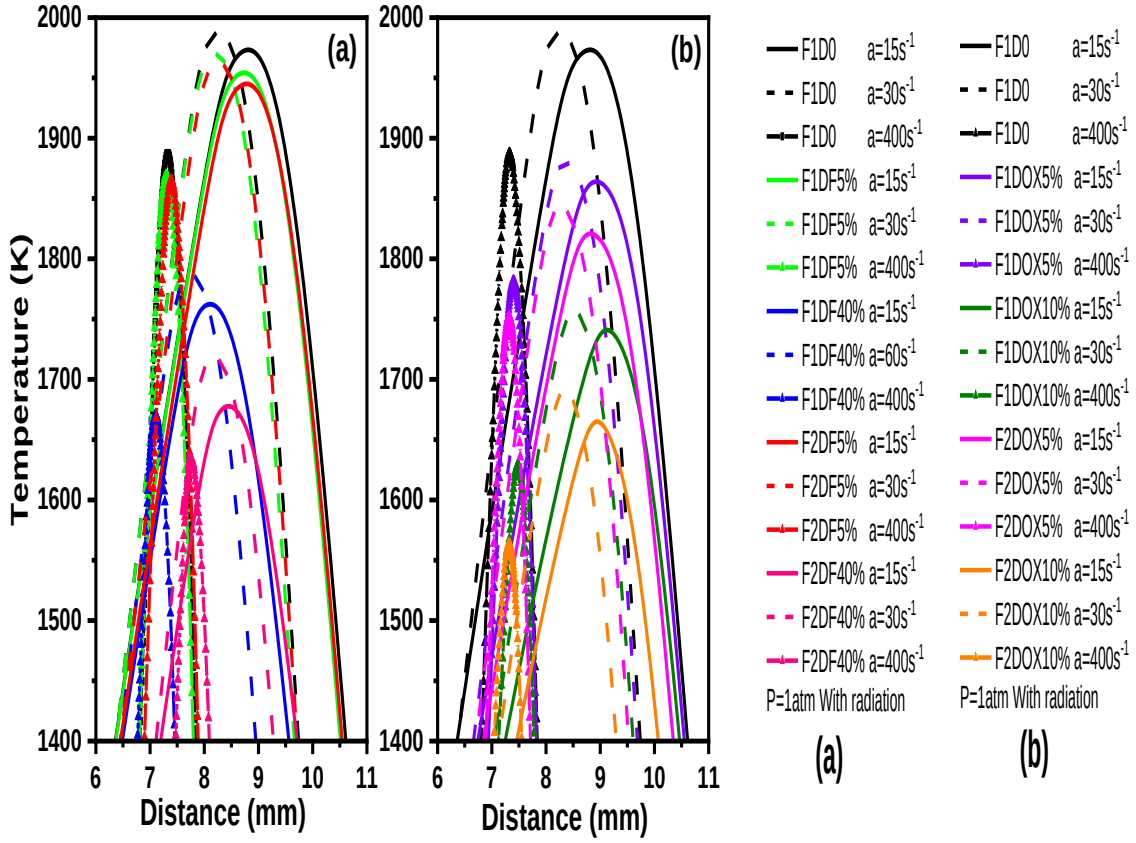

Figure 3. Distributions of flame temperature in B25S25/air counterflow diffusion flames with (F1) H_2O dilution and (F2) CO_2 dilution; (a) fuel side dilution, (b) oxidant side

Figure 3 shows the impact of the strain rate and the dilution by H2O and CO2 on the maximum flame temperature. These profiles highlight the similar influence of the parameters (a, H2O, and CO2) on the Tmax of the flame. We also note that the increase of these two parameters leads to a decrease in Tmax which meets one of our objectives. At first glance, these results show that the dilution on the fuel side has less effect on the reduction of the flame temperature than that on the air side, particularly at low concentrations (5%) of the two diluting agents Fig. 3(a, b). This the effect is clearly visible in fig. 4 and 5, in particular the last one, which allows us to see more precisely the effect of dilution and strain rate on the

Tmax of the mixture. dilution as a function of strain rate (a=15s^{-1}(solid line), a=30s^{-1}(dash line) and a=400s^{-1}(line + symbol)) and the distance from the fuel nozzle, D=1.5 cm, 300k.

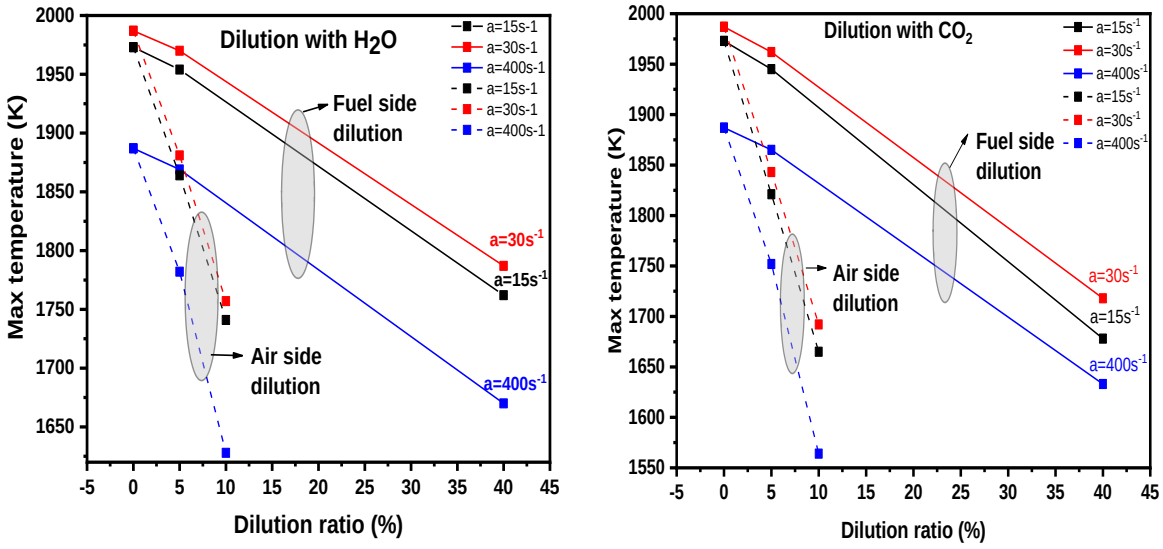

Figure 4. The peak of the maximum temperature of B25S25/air counterflow diffusion flames with the different dilution ratio of H_2O and CO_2 dilution on the air and fuel side, for different strain rates rate, D=1.5 cm, 300k.

Second, the results show that whether added to the air side or the fuel side, CO2 is more effective in lowering the flame temperature than H2O. This is mainly due to the greater heat capacity of CO2 than that of H2O. In addition to that, added diluents (H2O and CO2), contribute both thermally and chemically to the flame characteristics. Thermally, the addition of these diluents modifies the physical properties of the flame, such as its temperature. For example, the addition of H2O can cause a super adiabatic effect in the flame temperature due to its decomposition. Chemically, these diluents can influence the reactions that occur in the flame. For instance,

compared to the addition of CO2, the addition of H2O significantly enhances a certain reaction known as H+O2 → O+OH chain branching.

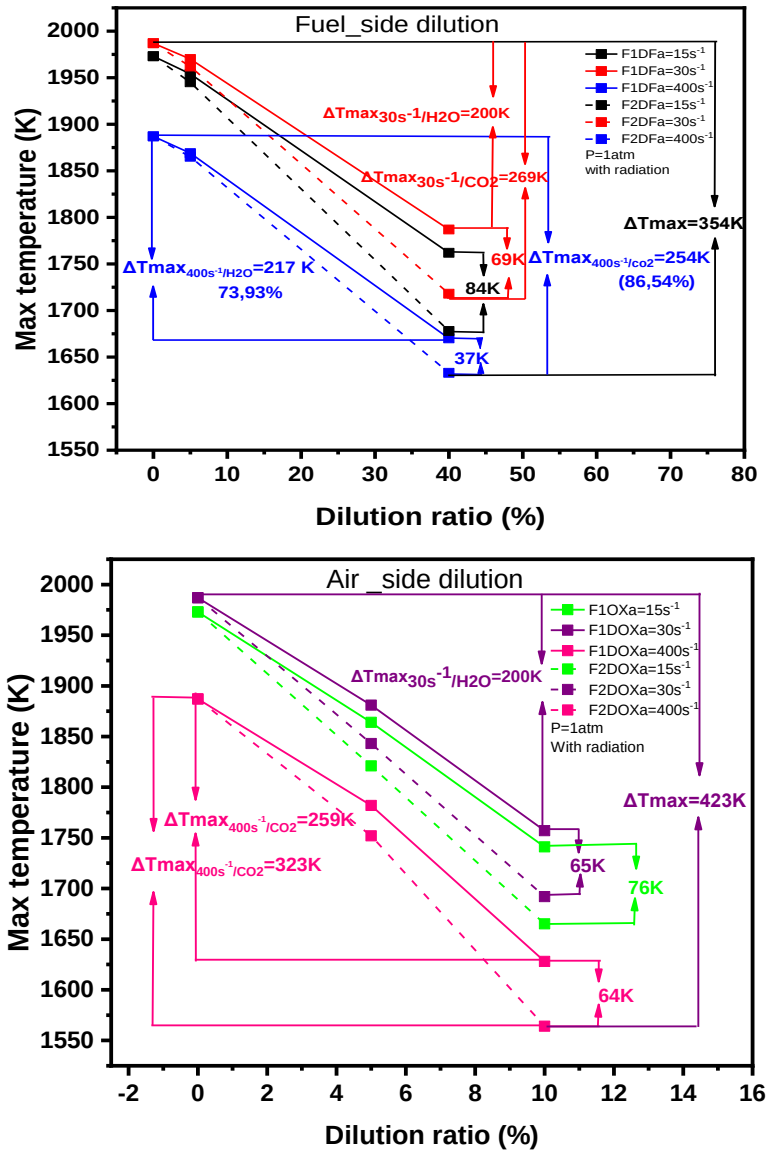

Figure 5. The differences in the peak flame temperature of B25S25/air counterflow diffusion flames as a function of the dilution ratio of H2O and CO2
and strain rate, D=1.5 cm, 300k.

Finally, concerning the location of the front of the flame which is considered to correspond to the stagnation plane and maximum temperature position, we observed in Fig. 3(a, b) that the H_2O fuel side dilution shifts the peak temperature slightly towards either the fuel nozzle but when H_2O added to the air side the peak of Tmax is always shifted toward the air nozzle. However, when added to the air stream, CO_2 dilution can slightly move the peak temperature toward the oxidizer

nozzle, but when CO_2 is added to the fuel side, we see that the peak of Tmax shifted slightly to the fuel duct except in the case of dilution with 40% of CO_2, where we note that the peak of the temperature moved to the oxidizer side. These changes are related to the relative molar weights of N_2, H_2O, and CO_2. The second factor that controls the location of the flame front is the stretching rate, when it rises, the flame front is displaced towards the fuel side.

Figure 6(a, b) presents the distributions of NO mole fraction as a function of strain rate, H_2O, and CO_2 dilution in the fuel and airside along the distance X between the two ducts. We note that there is a strong correlation between the effects of CO_2 and H_2O dilution and strain rate on flame temperature and NO mole fraction distributions. It is clear that increasing strain rates and concentration of the diluents CO_2 and H_2O, reduce the molar NO fraction considerably on the airflow side than on the fuel side. The CO_2 dilution, on the air side, reduces NO more than H_2O dilution as shown in Fig. 6(b), unlike fuel side dilution with H_2O Fig. 6(a). These findings are consistent with the results of [29]. Where in high concentrations (40%) in particular, we

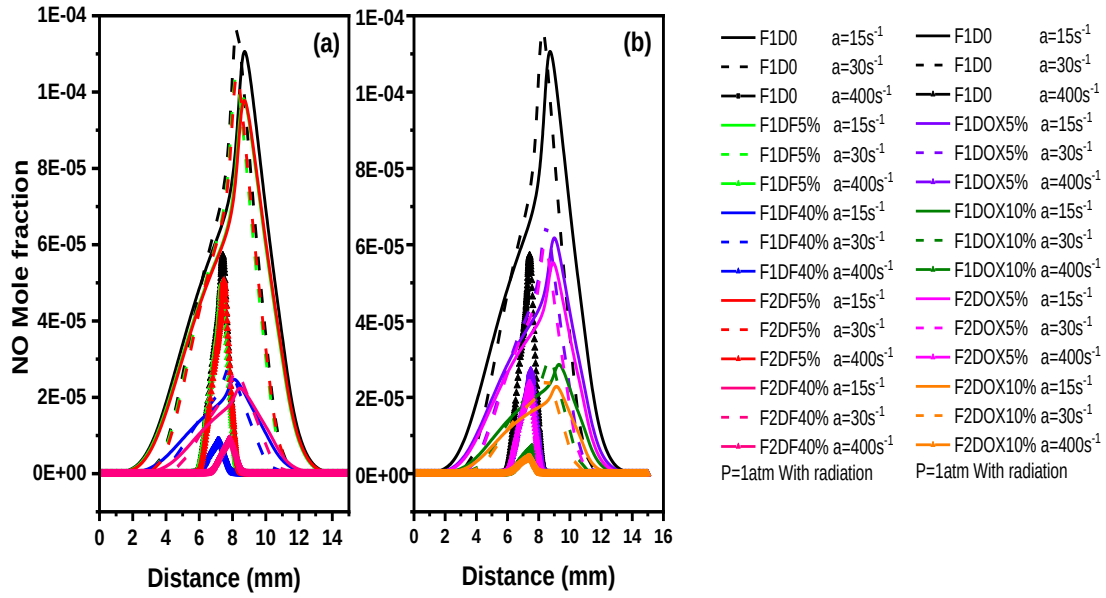

Figure 6. Distributions of X_{NO} in B25S25/air counterflow diffusion flames with (F1) H_2O dilution and (F2) CO_2 dilution; (a) fuel side dilution, (b) oxidant side dilution as a function of strain rate (a=15s^{-1}(solid line), a=30s^{-1}(dash line) and a=400s^{-1}(line + symbol)) and the distance from the fuel nozzle, D=1.5 cm, 300k.

noticed a slight predominance of H_2O, which is inconsistent with the distribution of the maximum flame temperature. This occurrence is explained by Figure 7, which compares the CH radical distribution with or without dilution by H_2O and CO_2 for different strain rates. Fig. 6 shows that

H_2O dilution has a stronger suppressive effect than CO_2 dilution on NO production because H_2O dilution on the fuel side limits CH radical's generation more than CO_2 and the first reaction of the prompt NO is slowed by the lower CH concentration in the fuel-side H_2O dilution, despite the higher temperature of the fuel-side CO_2 dilution than that of the fuel-side H_2O dilution. Since prompt NO is the predominant NO generation pathway, total NO emission is reduced.

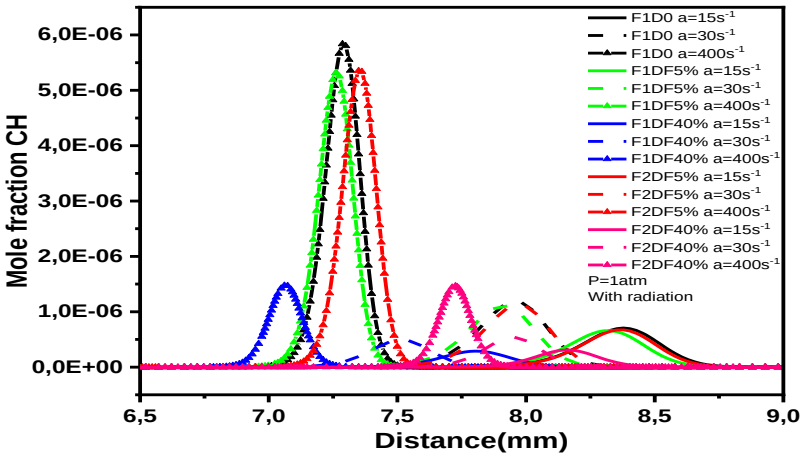

Figure 7. Distributions of CH mole fraction in B25S25/air counterflow diffusion flames with (F1) H_2O dilution and (F2) CO_2 dilution; (a) fuel side dilution as a function of strain rate ($a=15s^{-1}$(solid line), $a=30s^{-1}$(dash line) and $a=400s^{-1}$(line + symbol)) and the distance from the fuel nozzle, D=1.5 cm, 300k.

Strain rate, dilution, and radiation Effects on the maximum flame temperature

Figure 8 shows the evolution of the Tmax and extinction limits as a function of the strain rate for dilution by H_2O (denoted by F1) and CO_2 (denoted by F2). (Fig. 8 (a) fuel side and Fig. 8 (b) oxidizer side) with radiation at atmospheric pressure. For all cases, it is noticed that the maximum flame temperature increases initially, then decreases after taking its maximum with an increasing strain rate. Furthermore, the extinction points positions are shifted to the decreasing direction of the strain rate, regardless of the type, the amount, and the side of the dilution. This means that the extinction strain rate interval is globally reduced by dilution. At low strain rates, the reduction of maximum temperature is related to radiation heat loss. This trend becomes significant with the increase in the dilution percentage by volumes of CO_2 and H_2O since the radiation absorption coefficients for these diluents are high. At high strain rates, residence times are reduced and reactions are dominated by unburned effects [44], the reduction of the maximum flame temperature at high strain rates then follows the typical upper branch of the well-known S-curve.

Figure 8(a) shows profiles of the maximum temperature and extinction limits for different dilution volumes by H_2O (plain lines) and CO_2 (dashed lines) on the fuel side. Here, the equimolar composition of the fuel is diluted progressively by a diluent volume ranging from 0 to 40% according to equation (1). It is noted that the maximum temperature profiles have the same behavior for both cases of diluents. An increase in diluent volume reduces the fuel concentrations

which causes the T_{max} to drop principally by thermal effect, accordingly, the extinction intervals in the function of strain rate are reduced since the flame becomes weaker.

Quantitatively, the maximum of this temperature falls by 0.86%, from 1985K to 1968K when a dilution of 5% (F1DF5%) with H_2O is operated. Whereas, it reduces by 10%, from 1985K to 1790K with a dilution of 40% by H_2O (F1DF40%). On the other hand, for the same dilution percentages, the extinction strain rate drops from 1728 s^{-1} for the flame F1DF5% to 666 s^{-1} for the flame F1DF40% with a strain rate interval width of 1062 s^{-1}. When the dilution with CO_2 is practiced, the T_{max} is reduced by 1.1% for the flame F2DF5%, and by 14% for the F2DF40% one. The extinction strain rate varies from 1728 s^{-1} to 599 s^{-1} with an interval width of 1130 s^{-1}. It can be seen that CO_2 reduces temperature efficiently compared to H_2O; moreover, it enables a wide interval of operating strain rate values.

The dilution of the oxidizer side is presented in Figure 8(b). The effects of increasing volumes of the diluents (H_2O, CO_2) and the strain rate on T_{max} are presented. Globally, similar behavior to dilution on the fuel side is observed. However, it is noticed that combustion didn't occur for volumes of diluents more than 15% of oxidizer. Moreover, variations are steeper when increasing dilution. When adding 5% of H_2O to the oxidizer, the maximum temperature reduces by 5.4% (from 1985K in the case without dilution to 1883K for the flame F1DOX5%). If the volume of H_2O is increased to reach 15% in the oxidizer (F1DOX15%), then the maximum temperature falls by 20.3%, i.e., from 1985 to 1650K. The operating interval, in terms of extinction, goes from 1086 s^{-1} to 154 s^{-1}, i.e., 938 in width corresponds to 15% H_2O dilution. Now, if dilution with CO_2 of the oxidizer side is considered, the Tmax decreases by 7% for 5% dilution (F2DOX5%) and by 24% for 15% dilution (F2DOX15%). On the other hand, the extinction limits vary between 1000 s^{-1} and 25 s^{-1} which represent a strain rate interval width of 975s^{-1}.

Maximum flame temperature deviations without dilution and other cases (5% and 40% of H_2O and CO_2 for the dilution fuel side; and 5% and 15% of H_2O and CO_2 for the oxidant side dilution) are indicated in Figure 8.

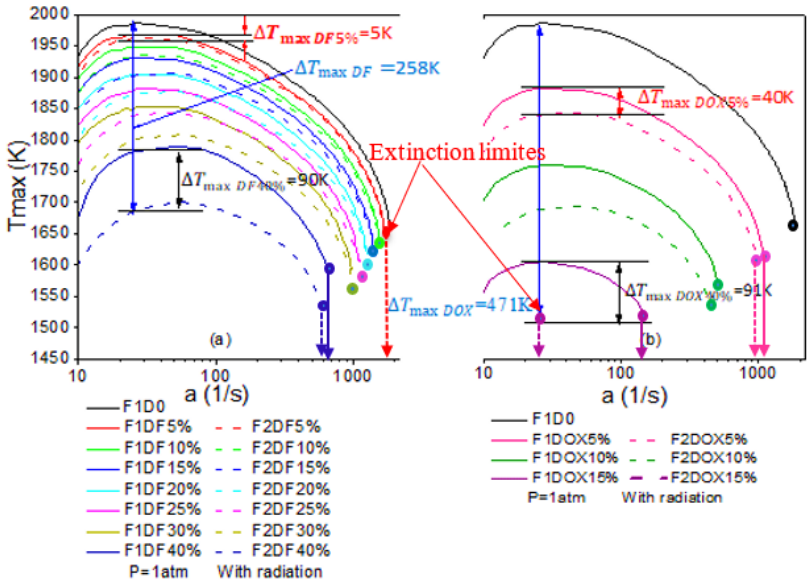

Figure 8. The maximum flame temperature and extinction limits in counterflow diffusion flames in the function of strain rate and dilution with H_2O (F1) and CO_2 (F2) dilution: (a) fuel side dilution and (b) oxidizer side dilution.

The radiation effect on Tmax is depicted in Figure 9. The strain rate was varied from ignition to extinction limits and dilution was operated by both H_2O (F1 flames in Figure 9 (A)) and CO_2 (F2 flames in Figure 9 (B)) on both fuel (Fig. 9 (A1) and Fig. 9 (B1)) and oxidizer (Fig. 9 (A2) and Fig. 9 (B2)) sides. In Figure 9, radiating flames are denoted by (R) whereas no radiating (adiabatic) ones by (NR). All flames exhibit similar behavior when radiating (dashed lines) and adiabatic (plain lines) are compared. In the low strain rate zone, the Tmax increases to reach its higher value and then drops to the extinction limit at the high strain rate. The temperature of the adiabatic flames increases with the rate of deformation which results in the supply of fuel; it is greater than that reached in radiant flames and this is for the same strain rate, which explains the presence of heat losses by radiation. For a certain value of strain rate, the difference between radiant and non-radiant flames reaches its maximum value and then decreases to zero in the region of high strain rates. In this region, the two curves meet because the flame is very thin and the radiation losses become negligible.

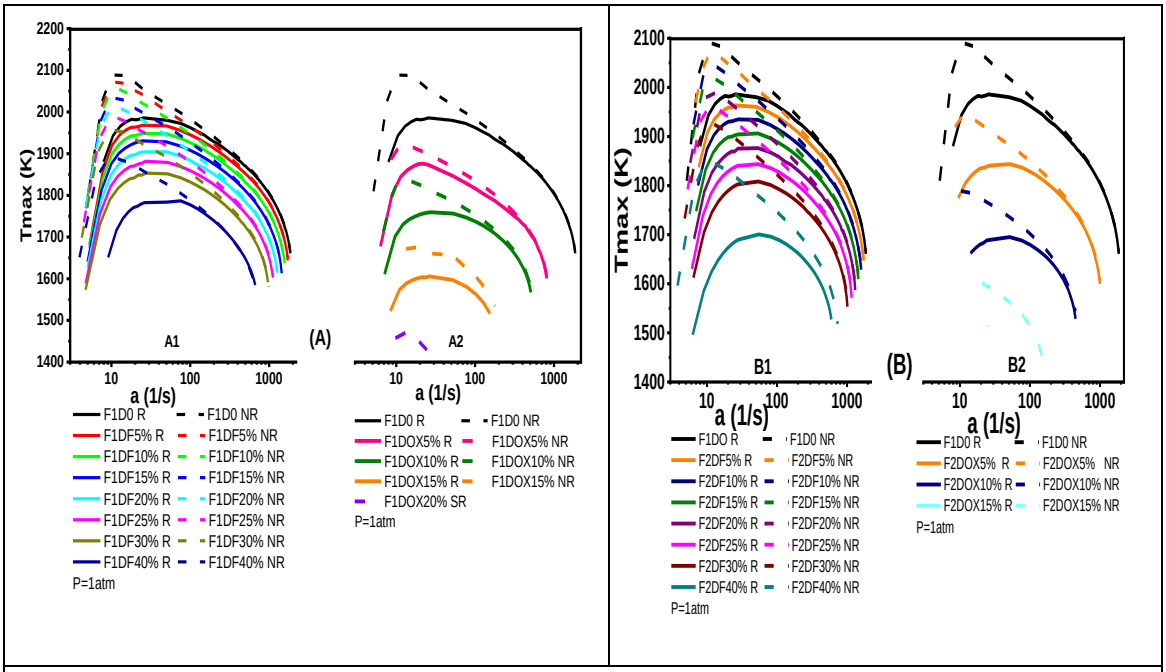

Figure 9. Effect of radiation, stretching rate, and dilution on the maximum temperature and the limits of ignition and extinction of B25S25/air counterflow diffusion flames with (F1) H_2O dilution and (F2) CO_2 dilution; fuel side dilution, oxidant side dilution as a function of strain rate, D=1.5 cm, 300K.

Quantitatively, for low strain rates, a < 300s^{-1}, the Tmax reaches a drop of 8% for the F2DF40% composition due to radiative heat loss. In this case, the fuel is diluted by 40% of CO_2, which is a highly radiating species. We record a decrease of T_{max} between [4.78%-5.45%] for dilution with 5% and 40% H_2O on the fuel side and a decrease between [2.03% - 4.35%] for dilution with 5% and 15% of H_2O on the oxidant side. The dilution on the fuel side, with 5% and 40% and with 5% and 15% of CO_2 on the airside, decreases the T_{max} between 5.12% - to 7.91% and 5.12%-5.43% respectively. At the time, the radiation heat losses decrease the T_{max} of B25S25 by 5.07%. This is because radiation heat losses are proportional to the reaction zone volume. In addition, as illustrated in Fig. 9, the thickness of the reaction zone is inversely related to the square root of the stretch rate. The radiation impact is eliminated for a > 300 s^{-1}, and hence the complicated thermophysical consequences due to radiation effects are also excluded. These results are consistent with previous research [25, 27, 29, 43]. As shown in Figures 9(A) and 9(B), the flame ignition limits decrease with the increase of the CO_2 and H_2O molar fractions. Thus, dilution improves the flammability of the mixture because of the high percentage of minority species (H, O, OH), resulting from the decomposition of the diluents, by improving thermal diffusion, reactivity, and resistivity of the flame. This is one of the advantages of dilution. It is also noted that the rate of deformation and the concentration of these diluents reduce the limits of extinction. Diluted flames, by H_2O on the fuel and oxidizing side, are more resistant to stretching speeds than those diluted by CO_2. This is explained by the decomposition of H_2O, which provides an increase in radicals such as H and OH. It is also observed that Tmax peaks, flames diluted with

H_2O or CO_2 without radiation, are moved to high stretching rates compared to those with radiation. In conclusion, the effects of dilution on the fuel side are much greater than radiant heat losses due to the high absorption coefficients of the species existing in the mixture such as (CH_4, CO_2, CO, and H_2O), and dilution with CO_2 is more efficient than dilution with H_2O.

As a result, it is found that the addition of CO_2 tends to reduce the flame temperature both thermally and chemically, but the addition of H_2O chemically promotes the reaction while thermally retaining it.

Effects of dilution and strain rate on OH, C_2H_2, C_2H_3, CO, NO, N_2O, and NO_2 (Oxy. and fuel side)

Figure 10 shows the evolution of the maximum of the OH, C_2H_2, and C_2H_3 radicals as a stretching rate function at the different dilutions with H_2O and CO_2 (a-fuel side and b- b-oxidant side). The OH radical is an indicator of the reactivity of the mixture, and the acetylene C_2H_2 also has very high reactivity. It is noted for these two radicals that, after ignition, the difference in the production of these radicals becomes visible as shown in Figures 10(A) and 10(B). The evolution of these radicals is not monotonous; its proportion increases to a maximum corresponding to the rate of stretching between $100s^{-1}$ and $300s^{-1}$ for the different concentrations of the diluents, and then it falls with the increase in the values of the stretching rate. We noted that when the mixture is diluted with H_2O, either on the oxidizer side or on the fuel side, the mixture is more productive of these OH and more resistant to stretching rates than when diluted with CO_2. This is logical since the chemical effect of H_2O promotes the formulation of OH by $H + O_2 = O + OH$ and $O + H_2O = 2OH$, but the chemical influence of CO_2 suppresses these processes and limits the maximum concentration of OH [26]. Therefore, the decomposition of H_2O represents a source of H and OH radicals that improve the resistance of flames to stretching, and they are considered sources of acetylene. This is what makes the dilution by H_2O concurrence that by CO_2 in its reduction. On the other hand, this species is very affected by the chemical effect of CO_2 [8]. This is what makes dilution by H_2O competes with that by CO_2; in the reduction of C_2H_3 because the C_2H_3 species is very Influenced by the chemical effect of CO_2 [8]. After a strain rate of $100s^{-1}$, a brisk increase is observed to a maximum of nearly $400s^{-1}$ and $900s^{-1}$ corresponding to the increase of the species C_2H_2 which is the precursor soot production; or recombined with hydrogen in maximum quantities as shown in Figures 10(A) and 10(B) by the reaction R $H+C_2H_2=C_2H_3+M$, and this explains the time shift that we see between graphs 10(A) and 10(B) relative to 10(C). Then there is a decrease until the flame is extinguished. In conclusion, it can be said that the results obtained contribute to a reduction in the quantity of Polycyclic Aromatic Compounds results (PAC).

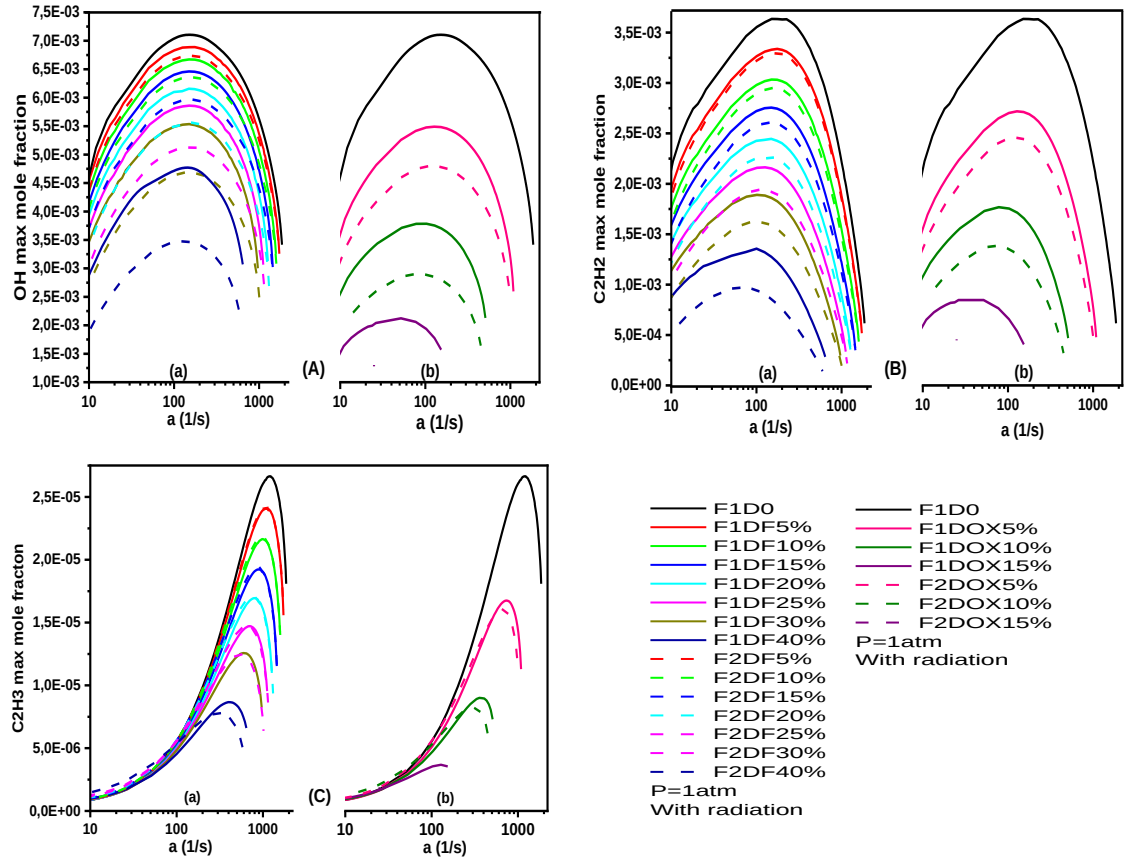

Figure 10. Distributions of (A) OH, (B) C_2H_2, and (C) C_2H_3 maximum mole fraction in B25S25/ air counter-current diffusion flames as a function of strain rate and dilution with H_2O (F1) and CO_2 (F2), fuel side, (a) and oxidizer side, (b), D = 1.5 cm, 300 K.

Figure 11 shows the variation of the maximum value of (Y_{CO}) as a function of the stain rate and dilution by H_2O and CO_2 (a- fuel side and b- b-oxidant side) with radiation at atmospheric pressure. The results show that the CO production rate decreases with the increase in H_2O and CO_2 concentrations. The mole fraction of CO, (Y_{CO}), shows small variations generated by the injection flow rate (stretch rate). This is because increasing the stretching velocity reduces the Damköhler number and residence time, thereby enhancing non-equilibrium effects that reduce Y_{CO}. What is interesting in these results is that the type of diluent does not affect the CO emission, especially for the fuel-side dilution for the same percentage of H_2O or CO_2. The variation of the maximum Y_{CO} value is the same quantitatively and qualitatively except for 40% of the diluents which is evaluated as Ymax (CODF40%) = 0.1298.

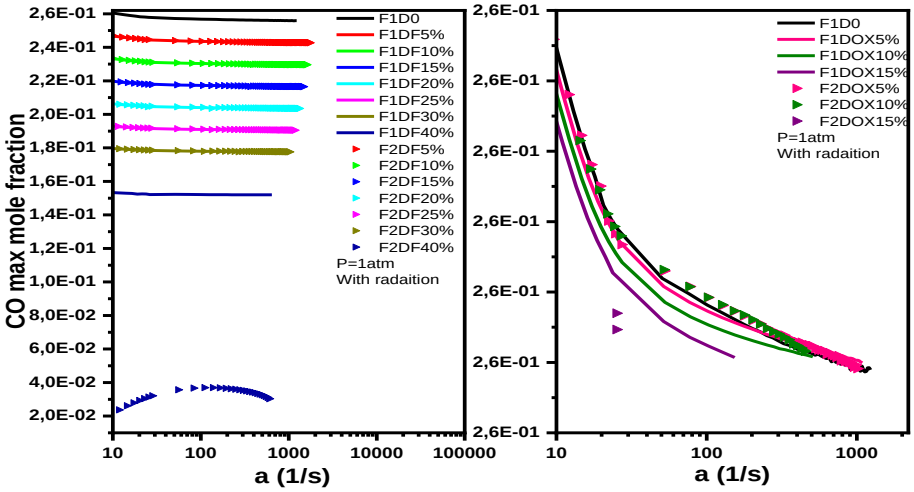

Figure 11. Distributions of CO maximum mole fraction in B25S25/air counterflow diffusion flames with (F1) H_2O dilution and (F2) CO_2 dilution; (a) fuel side dilution, (b) oxidant side dilution as a function of strain rate, D=1.5 cm, 300K.

The evolution of the maximum molar fraction of the noxious species NO and NO_2 are shown in Figures 12(A) and 12(B) respectively. Nitrogen dioxide is 40 times more toxic than (CO) and four times more toxic than NO. nitrous oxide of chemical formula N_2O is a powerful greenhouse gas that remains in the atmosphere for a long time (about 120 years). It is partly responsible for the destruction of the ozone represented in Fig 12(C). This colorless and non-flammable gas, coming essentially from the transformation of nitrogenous products, has the same variation pattern as (NOx) shown in Fig 12(A). It can be seen that the profiles show a non-monotonous behavior with the injection rate. they are similar to those of Tmax and OH radicals because the NO is very sensitive to high temperatures. The peak mole fractions, Y_{NO} and Y_{NO2}, shown in Figure 12, decreases with increasing strain rate and volume percent diluent. We notice that the

The Y_{N2O} peak is located between a= [$10s^{-1}$-$19s^{-1}$] and the Y_{NO} peak is located between a=[$25s^{-1}$-$50s^{-1}$]. Therefore, this shift is explained by the consumption of N_2O to production NO. Note that, also, the diluent type does not affect the N_2O emission in the fuel-side dilution with concentrations less than 40%, see Figures 12(aA), (aB), and (aC). Dilution with CO_2, on the bending side, is the most effective in reducing these emissions. In addition, compared to undiluted, the molar production rates of nitrogenous species are significantly reduced. Indeed, the dilution by 5% of H_2O, a reduction of NO of 12.72% is recorded for the dilution on the fuel side and of 31.55% on the oxidizing side; this is located at a= $25s^{-1}$. Then the flame has a higher resistance on the combustible side than on the oxidizing side. the dilution by 10% of CO_2, on the oxidant side, represents the best composition since the flame F2DOX10% is more stable and resistant than that of the F2DOX15% flame. A reduction in NO of 97% is obtained for a=$50s^{-1}$. In this study, the formation of NOx on the fuel side and the thermal path is suppressed for the dilutions of 40% on the fuel side and 10% on the oxidizer side. We see that the dilution of CO_2 is more effective than that of H_2O, especially on the oxidizing side. Finally, it is noted that the NOx emissions of

mixtures diluted on the fuel side by CO_2 are greater, whereas those diluted by H_2O on the fuel side emit more NOx. Therefore, the overall NO emission in the case of H_2O addition is higher than that in the case of CO_2 addition.

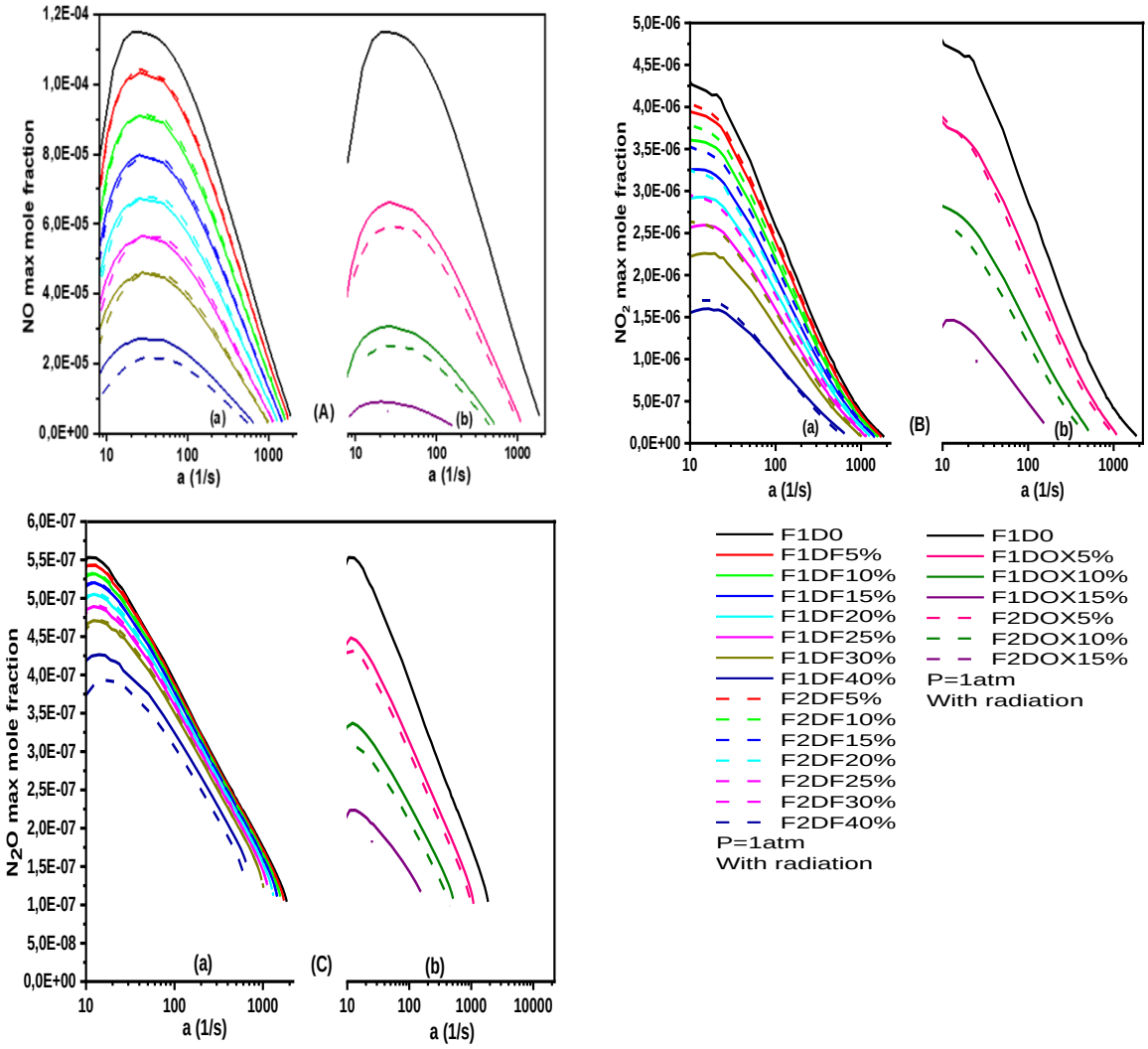

Figure 12. Distributions of (A) NO, (B) NO_2 et (C) N_2O maximum mole fraction in B25S25/air counterflow diffusion flames with (F1) H_2O dilution and (F2) CO_2 dilution; (a) fuel side dilution, (b) oxidant side dilution versus strain rate, D=1.5 cm, 300k

Conclusion

This numerical study was carried out, on a counter-flux diffusion flame of the fuel mixture (biogas-Syngas/air), to clearly show the contributions of diluents (H_2O and CO_2), the strain rate varying from the ignition limit to the extinction limit, and the effect of radiation on the flame structure and emission characteristics of NO and CO. The main conclusions are as follows

- Dilution by H_2O and CO_2 reduces the maximum flame temperature and consequently the emissions of NO_x, CO, C_2H_2, and other soot whatever the side of dilution; this reduction effect becomes much more important with increasing volume percent of CO_2 and H_2O.
- H_2O and CO_2 have the same radiative effect.

- H_2O and CO_2 have the same radiative effect.
- Carbon dioxide, whether added on the airside or the fuel side, is more effective than H_2O in reducing the maximum flame temperature, due to its high heat capacity and its chemical effect.
- The effect of dilution is stronger than that of the strain rate on the reduction of the maximum temperature.
- The increase in the concentration of diluents reduces the extinction limits and negatively affects the resistance of the flames because the ignition limits are favored. An advantageous result is then obtained.
- The maximum temperatures and extinction limits i.e., flame resistance for the fuel-side dilution are higher than those for the oxidant-side dilution; nevertheless, the latter is still preferred in applications not requiring a high injection velocity, because according to the results, we approach zero-emission for 10% of the CO_2 dilution.
- The molar production rates of the nitrogen species are significantly prevented where for $a=50s^{-1}$ and for the dilution on the fuel side a NO diminution of 77% for 40% H_2O and 81% for 40% CO_2 is reached, for the dilution on the oxidant side a reduction of 92.12% for 15% H_2O and 97% for 15% CO_2. In this study, the formation of NO_x by fuel and thermal routes is suppressed for the dilutions of 40% fuel and 10% oxidant.

References:

1. Watson, G.M., J.D. Munzar, and J.M. Bergthorson, *NO formation in model syngas and biogas blends.* Fuel, 2014. **124**: p. 113-124.
2. Wang, L., et al., *Physical and chemical effects of CO2 and H2O additives on counterflow diffusion flame burning methane.* Energy & fuels, 2013. **27**(12): p. 7602-7611.
3. Xu, H., et al., *Effects of H2O and CO2 diluted oxidizer on the structure and shape of laminar co-flow syngas diffusion flames.* Combustion and Flame, 2017. **177**: p. 67-78.
4. Guethe, F., M. de la Cruz Garci´ a, and A. Burdet. *Flue gas recirculation in gas turbine: Investigation of combustion reactivity and NOx emission.* in *Turbo Expo: Power for Land, Sea, and Air.* 2009.
5. Shi, B., et al., *Effects of internal flue gas recirculation rate on the NOx emission in a methane/air premixed flame.* Combustion and Flame, 2018. **188**: p. 199-211.
6. Liu, H., et al., *Effect of FGR position on the characteristics of combustion, emission and flue gas temperature deviation in a 1000 MW tower-type double-reheat boiler with deep-air-staging.* Fuel, 2019. **246**: p. 285-294.
7. Park, J., et al., *A Study on Flame Structure and NO Emission in FIR-and FGR-applied Methane-air Counterflow Diffusion Flames.* Journal of the Korean Society of Combustion, 2016. **21**(1): p. 38-45.
8. Strakey, P., N. Weiland, and G. Richards, *Combustion Strategies for Syngas and High-Hydrogen Fuel.* The Gas Turbine Handbook, 2006.

9. Hadef, A., et al., *Impact de l'étirement sur la structure thermochimique d'une flamme de diffusion d'un biogaz hydrogéné en régime sans flamme.* Revue des Energies Renouvelables, 2016. **19**(3): p. 367-376.
10. Javed, M.T., N. Irfan, and B. Gibbs, *Control of combustion-generated nitrogen oxides by selective non-catalytic reduction.* Journal of environmental management, 2007. **83**(3): p. 251-289.
11. Locci, C., et al., *Selective non-catalytic reduction (SNCR) of nitrogen oxide emissions: a perspective from numerical modeling.* Flow, Turbulence and Combustion, 2018. **100**(2): p. 301-340.
12. Sattelmayer, T., et al., *NOx-abatement potential of lean-premixed GT combustors.* 1998.
13. Leonard, G. and J. Stegmaier, *Development of an aeroderivative gas turbine dry low emissions combustion system.* 1994.
14. Lee, C., et al., *Numerical study on effect of CO_2 addition in flame structure and NOx formation of CH4-air counterflow diffusion flames.* International Journal of Energy Research, 2001. **25**(4): p. 343-354.
15. Mazas, A., D. Lacoste, and T. Schuller. *Experimental and numerical investigation on the laminar flame speed of CH4/O2 mixtures diluted with CO2 and H2O.* in *Turbo Expo: Power for Land, Sea, and Air*. 2010.
16. Mazas, A., et al., *Effects of water vapor addition on the laminar burning velocity of oxygen-enriched methane flames.* Combustion and Flame, 2011. **158**(12): p. 2428-2440.
17. Li, Y.-H., et al., *Effects of flue gas recirculation on the premixed oxy-methane flames in atmospheric condition.* Energy, 2015. **89**: p. 845-857.
18. Bhargava, A., et al., *An experimental and modeling study of humid air premixed flames.* J. Eng. Gas Turbines Power, 2000. **122**(3): p. 405-411.
19. Park, J., S.I. Keel, and J.H. Yun, *Addition effects of H2 and H2O on flame structure and pollutant emissions in methane–air diffusion flame.* Energy & Fuels, 2007. **21**(6): p. 3216-3224.
20. Guo, H., W.S. Neill, and G.J. Smallwood, *A numerical study on the effect of water addition on NO formation in counterflow CH4/air premixed flames.* Journal of Engineering for Gas Turbines and Power, 2008. **130**(5).
21. Matynia, A., et al., *Comparative study of the influence of CO2 and H2O on the chemical structure of lean and rich methane-air flames at atmospheric pressure.* Combustion, Explosion, and Shock Waves, 2009. **45**(6): p. 635-645.
22. Liu, F., J.-L. Consalvi, and A. Fuentes, *Effects of water vapor addition to the air stream on soot formation and flame properties in a laminar coflow ethylene/air diffusion flame.* Combustion and flame, 2014. **161**(7): p. 1724-1734.
23. Hadef, A., et al., *Effect of Replacement of Air N2 by H2O on Internal Structure and Pollutants Formation in an Opposed jet Diffusion Combustion of a Hydrogenated Biogas in Flameless Regime.* Journal of Applied Fluid Mechanics, 2019. **12**(2 (Special Issue)): p. 19-28.
24. Ren, F., et al., *Numerical investigation on the effect of CO2 and steam for the H2 intermediate formation and NOX emission in laminar premixed methane/air flames.* International Journal of Hydrogen Energy, 2020. **45**(6): p. 3785-3794.

25. Park, J., et al., *Chemical effect of diluents on flame structure and NO emission characteristic in methane-air counterflow diffusion flame.* International Journal of Energy Research, 2002. **26**(13): p. 1141-1160.
26. Kim, S.G., J. Park, and S.I. Keel, *Thermal and chemical contributions of added H2O and CO2 to major flame structures and NO emission characteristics in H2/N2 laminar diffusion flame.* International Journal of Energy Research, 2002. **26**(12): p. 1073-1086.
27. Hwang, D.J., et al., *Numerical study on flame structure and NO formation in CH4–O2–N2 counterflow diffusion flame diluted with H2O.* International journal of energy research, 2004. **28**(14): p. 1255-1267.
28. Yang, K.-H. and H.-Y. Shih, *NO formation of opposed-jet syngas diffusion flames: Strain rate and dilution effects.* International Journal of Hydrogen Energy, 2017. **42**(38): p. 24517-24531.
29. Xu, H., et al., *A detailed numerical study of NOx kinetics in counterflow Methane diffusion flames: effects of fuel-side versus oxidizer-side dilution.* Journal of Combustion, 2021. **2021**.
30. Hwang, D.J., et al., *Numerical study on NO formation in CH4–O2–N2 diffusion flame diluted with CO2.* International journal of energy research, 2005. **29**(2): p. 107-120.
31. Shih, H.-Y., *Computed extinction limits and flame structures of H2/O2 counterflow diffusion flames with CO2 dilution.* International journal of hydrogen energy, 2009. **34**(9): p. 4005-4013.
32. Cao, Z.-j. and T. Zhu, *Chemical effects of CO2 dilution on flame structure and NO formation properties in methane-preheated air counterflow diffusion flame.* J. Combust. Sci. Technol, 2012. **18**: p. 123-130.
33. Gascoin, N., Q. Yang, and K. Chetehouna, *Thermal effects of CO2 on the NOx formation behavior in the CH4 diffusion combustion system.* Applied Thermal Engineering, 2017. **110**: p. 144-149.
34. Yang, J., et al., *Dilution effects of N2 and CO2 on flame structure and reaction characteristics in CH4/O2 flames.* Experimental Thermal and Fluid Science, 2019. **108**: p. 16-24.
35. Mameri, A., et al., *Combustion characterization of the mixtures biogas-syngas, strain rate and ambient pressure effects.* International Journal of Hydrogen Energy, 2019. **44**(39): p. 22478-22491.
36. Zouagri, R., et al., *Characterization of the combustion of the mixtures biogas-syngas at high strain rates.* Fuel, 2020. **271**: p. 117580.
37. Mameri, A., S. Boussetla, and A. Hadef, *A Two-Dimensional Simulation of Opposed Jet Turbulent Diffusion Flame of the Mixture Biogas-Syngas*, in *Advances in Renewable Hydrogen and Other Sustainable Energy Carriers*. 2021, Springer. p. 61-67.
38. Boussetla, S., A. Mameri, and A. Hadef, *NO emission from non-premixed MILD combustion of biogas-syngas mixtures in opposed jet configuration.* International Journal of Hydrogen Energy, 2021. **46**(75): p. 37641-37655.
39. Benbouaziz, O., et al., *Characterization of Biogas-Syngas Turbulent MILD Combustion in the Jet in Hot Co-Flow Burner.* Journal of Applied Fluid Mechanics, 2021. **14**(6): p. 1851-1868.
40. Chelliah, H., et al. *An experimental and theoretical investigation of the dilution, pressure and flow-field effects on the extinction condition of methane-air-nitrogen diffusion flames.* in *Symposium (International) on Combustion*. 1991. Elsevier.

41. Kee, R.J., et al. *A computational model of the structure and extinction of strained, opposed flow, premixed methane-air flames*. in *Symposium (International) on Combustion*. 1989. Elsevier.
42. Lim, J., J. Gore, and R. Viskanta, *A study of the effects of air preheat on the structure of methane/air counterflow diffusion flames.* Combustion and flame, 2000. **121**(1-2): p. 262-274.
43. Ju, Y., et al., *On the extinction limit and flammability limit of non-adiabatic stretched methane–air premixed flames.* Journal of fluid mechanics, 1997. **342**: p. 315-334.
44. Mameri, A. and F. Tabet, *Numerical investigation of counter-flow diffusion flame of biogas–hydrogen blends: Effects of biogas composition, hydrogen enrichment and scalar dissipation rate on flame structure and emissions.* International journal of hydrogen energy, 2016. **41**(3): p. 2011-2022.